

## FREE CONVECTION LIMIT TO HEAT TRANSFER FROM HEAT SINKS WITH SQUARE FINS ON A HORIZONTAL BASE Comparison with Cylindrical Fins

by

**Subhas Chandra HALDAR\* and Saurav MANNA**

Department of Mechanical Engineering, Haldia Institute of Technology,  
Haldia, India

Original scientific paper  
DOI:10.2298/TSCI121004133H

*Free convection about a single vertically orientated square fin on a horizontal plate has been investigated numerically. Fluid is drawn towards the fin from the far field which cools the fin and finally leaves through the top. For short fins, convection rather than the conduction is the controlling mechanism and this renders the fin thermal conductivity a parameter of little importance for such fins. Heat flux at the base of the fin decreases with increasing width of the fin confirming the benefits of large number of slender fins. A correlation has been developed to evaluate the heat flux at fin base which may be used to predict the upper bound of free convection heat transfer from any heat sink with square fins on a horizontal base. Rate of heat transfer so calculated has been compared with experimental data published recently. The study also reveals the advantage of the cylindrical fins over square fins.*

*Key words: free convection, natural convection, pin fin, square fin, heat sink, thermal management*

### Introduction

Use of fins is the most widely employed technique to increase the rate of heat transfer from a surface in many engineering applications and hence the topic was researched quite extensively. Increasing power densities of electronic components due to continuous miniaturization has maintained this research. An infinite number of combinations are possible amongst the heat sink base plate area, number of fins, thickness, length, spacing, and thermal conductivity of the fins and also the arrangement of the fins on the plate. This is another reason responsible for large number of reported studies on the topic. Free convection heat transfer is additionally influenced by the orientation of the fins. Plate fins forming an array of parallel channels, pin fins of square and circular cross-sections are the ones most widely used. While the fluid may impinge on the base plate or flow parallel to the base. Though cooling by forced convection is the dominant practice, natural convection is preferred for low power applications due to its reliability, noise-free operation, and energy saving. Additionally, in the event of failure of the fan, the component is left to cool by natural convection only. In order to be brief, recent articles on heat sinks with square and circular fins will be cited here. Kim *et al.* [1] carried out experiments to compare heat sinks with plate fins and with square fins cooled by impinging flow and did not

---

\* Corresponding author; e-mail: schaldar@rediffmail.com

observe the superiority of one over the other within the entire range of dimensions and flow velocities. Li *et al.* [2] selected a heat sink made of rectangular pin elements and cooled by confined impinging jet. They numerically studied the effects of Reynolds number, fin size, number of fins, position of the upper confining plate, fin thermal conductivity and nozzle to heat sink distance. In the article by Kim *et al.* [3], treated the array of pin fins cooled by parallel flow as porous medium and simplified the turbulent transport equations using volume averaging technique. Yang *et al.* [4] conducted experiments on twelve heat sinks comprising of pin fins of circular, square, and elliptic cross-sections. Aihara *et al.* [5] reported an experimental study on pin fin heat sink with a vertically oriented isothermal base plate. Zografos and Sunderland [6] concluded from their experiments on free convection cooling of heat sinks that pin fins are better than plate fins and the optimum center to center spacing is three times the diameter of the pin fin. Sahray *et al.* [7] investigated the effect of fin spacing on free convection heat transfer from a horizontal base with array of pin fins having square cross-section and fixed height. Kobus and Oshio [8] considered vertically oriented heat sink having circular pin fins cooled by combined convection with impinging flow. However, the major shortcoming is the assumption of uniform heat transfer coefficient over the entire surface of each fin as well as the free area of the base plate. Sahiti *et al.* [9] experimentally observed a large increase in forced convection heat transfer with circular pin elements mounted on a tube over its value for the bare tube. Huang *et al.* [10] performed experiments to determine the effect of orientation for free convection cooling of seven different heat sinks with square fins. They concluded that the upward facing orientation is better for finning factor, defined as the ratio of total wetted area to the base surface area, greater than 2.7 and finning factor rather than fin porosity plays a more important role in determining the rate of heat transfer. They also provided a correlation to estimate the rate of heat transfer as a function of heat sink geometries and Rayleigh number. Sahray *et al.* [11] performed experiments on cooling of horizontal base heat sinks with square fins by free convection and radiation. They too developed a correlation to predict free convection heat transfer from heat sinks with square fins oriented vertically upward.

To summarize the discussion on the literatures, the optimum fin spacing was found to be about three times the fin diameter which corresponds to a void fraction of approximately 90%. The correlations reported in two relatively recent articles [10, 11] to predict free convection heat transfer from heat sinks with square

pins provide significantly different values. Another important point which has not been emphasized in the published literature on heat sinks is the positive effects of curvature of cylindrical fins over square fins on heat transfer. This paper attempts to address the above shortcomings.

### Problem description

The present study deals with free convection heat transfer from a single pin element of square cross-section attached to a horizontal base. Figure 1 presents the schematic of the problem. A fin of square cross-section having width  $D$  and length  $L$  is attached to a horizontal base plate. The chosen co-ordinate system has

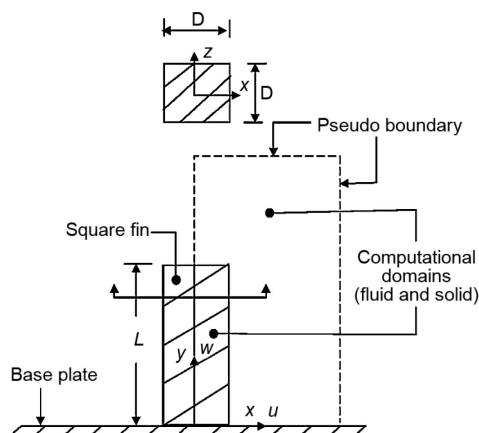


Figure 1. Schematic of the physical problem and the computational domain

its origin at the fin center on the base plate. The axial co-ordinate is  $y$  and the lateral co-ordinates are  $x$  and  $z$ . The direction of gravitational acceleration has been shown in fig. 1. The base of the fin was considered isothermal. In order to study the contribution to heat transfer by the fin alone, the unfinned area of the plate was assumed adiabatic.

The single fin results are then employed to predict the upper limit to free convection heat transfer from any heat sink with array of square pin elements oriented vertically upward. Finally, the heat sinks with square fins are compared with those consisting of cylindrical fins.

### Governing equations and boundary conditions

For obvious reasons, temperature variation on the fin surface is much greater along the axial direction ( $y$ -axis) than the lateral one ( $z$ -axis). This renders it essentially a 2-D ( $x, y$ ) phenomenon. The computational domain, marked in fig. 1, includes two different matter states; the solid fin and the fluid around the fin. For the fin, only the conduction equation needs to be considered. While for the fluid region, the governing equations are the conservation of mass, energy, and lateral and axial components of momentum. The mass and momentum conservation equations have been recast in terms of vorticity and stream-function applying Boussinesq's approximation for the buoyancy term. The governing equations in dimensionless variables, as defined in the nomenclature alongside the corresponding dimensional ones, are stated next:

$$\text{-- for fin} \quad \frac{\partial^2 t}{\partial x^2} + \frac{\partial^2 t}{\partial y^2} = 0 \quad (1)$$

In order to solve this equation, temperature conditions need to be specified on the fin boundaries and these are  $t = 1.0$  at the fin base,  $k_{\text{fin}}(\partial t/\partial x)|_{\text{fin}} = k_{\text{fluid}}(\partial t/\partial x)|_{\text{fluid}}$  at the vertical boundary of the fin,  $k_{\text{fin}}(\partial t/\partial y)|_{\text{fin}} = k_{\text{fluid}}(\partial t/\partial y)|_{\text{fluid}}$  at the fin tip and  $\partial t/\partial x = 0$  at the fin center line.

$$\text{-- for fluid} \quad u \frac{\partial \Omega}{\partial x} + w \frac{\partial \Omega}{\partial y} = \left[ \frac{\partial^2 \Omega}{\partial x^2} + \frac{\partial^2 \Omega}{\partial y^2} \right] - \text{Gr} \frac{\partial t}{\partial x} \quad (2)$$

$$-\Omega = \frac{\partial^2 \psi}{\partial x^2} + \frac{\partial^2 \psi}{\partial y^2} \quad (3)$$

$$u \frac{\partial t}{\partial x} + w \frac{\partial t}{\partial y} = \frac{1}{\text{Pr}} \left( \frac{\partial^2 t}{\partial x^2} + \frac{\partial^2 t}{\partial y^2} \right) \quad (4)$$

The stream-function and the two velocity components are related by:

$$u = \frac{\partial \psi}{\partial y} \quad \text{and} \quad w = -\frac{\partial \psi}{\partial x} \quad (5)$$

In order to facilitate numerical computation, pseudo boundaries were considered as indicated in fig. 1. Locations of both the vertical and horizontal pseudo boundaries were chosen far enough from the fin so as not to influence the results of the numerical solution. The fluid was deemed to cross the pseudo boundary surfaces orthogonally. The boundary conditions for the fluid region are then considered.

*Vertical fin surface:*  $\psi = 0$  and eq. (3) reduces to  $\Omega = -\partial^2\psi/\partial x^2$ . Temperature boundary condition on this surface has been stated before.

*Fin tip:*  $\psi = 0$  and eq. (3) becomes  $\Omega = -\partial^2\psi/\partial y^2$ . The thermal condition on this surface has already been specified.

*Free area of the plate:*  $\psi = 0$  and eq. (3) reduces to  $\Omega = -\partial^2\psi/\partial y^2$ . It may be recalled that the free area of the plate was assumed adiabatic in order to study the performance of the fin alone and accordingly  $\partial t/\partial y = 0$ .

*Vertical pseudo boundary:* The condition of orthogonal flow across this boundary results to  $\partial\psi/\partial x = \partial^2\psi/\partial x^2 = 0$  and also  $\partial\Omega/\partial x = 0$ . Fluid enters the computational domain at the free stream temperature and this is described mathematically as  $t = 0$  if  $u < 0$ . While the fluid leaves this boundary, identified by  $u > 0$ , with  $\partial t/\partial x = 0$ .

*Horizontal pseudo boundary:* Orthogonal flow dictates  $\partial\psi/\partial y = \partial^2\psi/\partial y^2 = 0$  and  $\partial\Omega/\partial y = 0$ . Temperature conditions on this surface are  $\partial t/\partial y = 0$  if  $w > 0$  (outflow) and  $t = 0$  if  $w < 0$  (inflow).

*Fin center line:* Symmetry demands  $\partial\psi/\partial x = \partial t/\partial x = 0$  as well as  $\Omega = 0$ .

## Numerical method

The governing dimensionless equations were solved in conservative form by finite difference technique based on control volume discretization over non-staggered grids. The equations were discretized following the cell average QUICK scheme [12] which is expected to produce grid-independent results with fewer grids when compared to second order upwinding [13]. However, the wall adjacent cells were discretized by central differencing due to absence of the adjoining cells on one side.

Solution was initiated with dimensionless temperature as zero everywhere within the computational domain except at the base of the fin. Equation (1) was solved to obtain the temperature distributions within the fin which were then substituted in the discretized form of the temperature boundary conditions to update the temperature values at the boundary nodes of the fin. Next the eq. (4) for  $t$ , eq. (2) for  $\Omega$ , eq. (3) for  $\psi$ , and eq. (5) for velocities  $u$  and  $w$  from  $\psi$  were solved in the fluid region. Vorticity values at the fluid boundary were then updated satisfying the respective boundary conditions and this completes one cycle. The cycle was reiterated till a converged solution was achieved.

Individual equations were converged to 0.0001%. Global convergence was assessed on vorticity since it was found to be more sensitive. Global convergence was deemed achieved when the differences of vorticity values at each grid point between two consecutive iteration cycles were less than 0.001%.

**Table 1. Effect of grid spacing on the rate of heat transfer**

	(a) Varying $x$ -spacing				(b) Varying $y$ -spacing			
$x$ -spacing	0.04	0.02	0.01	0.005	0.01	0.01	0.01	0.01
$y$ -spacing	0.01	0.01	0.01	0.01	0.04	0.02	0.01	0.005
Rate of heat transfer, $q$	7.808	7.437	7.291	7.243	7.302	7.306	7.291	7.313

Spacing along each co-ordinate direction was varied while keeping the other spacing fixed. Some representative results are shown in tab. 1. The spacing along  $x$ -direction was found to have more influence on the results. Numerical accuracy was found to be better with uniform

The program was solved with various pairs of radial and axial grid spacing in order to arrive at suitable values of them producing grid-independent results.

rather than non-uniform spacing. A spacing of 0.01 in both x and y co-ordinates was chosen to generate further results.

In order to arrive at proper locations of the two pseudo boundaries, the results were generated by shifting one boundary at a time while keeping the other at a fixed location. As expected, the influence of these two boundaries is observed to weaken with increasing distance from the fin. The vertical boundary at an  $x$ -value of 1.0 and the horizontal boundary at an  $y$ -value of 1.2 were accepted for further calculations since the changes in heat transfer values are not significant if these boundaries are shifted farther away from the fin.

There are three ways to numerically determine the rate of heat transfer from the fin; conduction across the base of the fin, convection from the fin surface, and the heat carried away by the fluid. Theoretically all the three values are equal at steady-state. The maximum deviation amongst these three numerically calculated values was found to be less than 0.1% and this validates the accuracy of the computational code.

### Results and discussions

Results were generated for Grashof number based on fin length within the range of  $10^2$  to  $10^6$ , fin to fluid thermal conductivity ratio from 2000 to 20000, and fin diameter to length ratio from 0.02 to 0.5. These ranges cover the fin dimensions, fin materials and operating temperatures encountered in most heat sink applications. The fluid around the fin was chosen as air by specifying a Pr value of 0.7 in eq. (4).

The effect of fin thermal conductivity on the rate of heat transfer from the fin will be scrutinized first. Figure 2 plots the rate of heat transfer from the fin as a function of its diameter to length ratio for the two extreme values of fin to fluid thermal conductivity ratio *i. e.*  $2 \cdot 10^3$  and  $2 \cdot 10^4$ . It confirms the fact that fins of higher thermal conductivity offers better heat transfer. Additionally, the figure reveals that the advantage of higher thermal conductivity gradually fades away with the increase in fin diameter. The heat is conducted into the fin from the plate and then transferred to the surrounding fluid by convection at the fin surfaces. The weaker of the two mechanisms will control the rate of heat transfer. Now, conduction heat transfer across the fin base is proportional to the square of the fin width while the convection heat transfer at the fin surface is proportional to just the fin width (ignoring the tip due to its small contribution to heat transfer). As a consequence, convection becomes weaker of the two with increasing fin width and hence the controlling mode. With convection as the controlling mode for fins with large width, the fin thermal conductivity which is associated with conduction becomes a parameter of little significance. This explains the convergence of the two profiles with increasing fin width, fig. 2.

Hereafter results have been presented for fin to fluid thermal conductivity ratio of  $10^4$  which approximately equals to that of aluminum alloys, the materials most widely used for heat sinks, to air.

In order to observe the flow pattern, the velocity vectors for the case of  $D/L = 0.2$  and  $Gr = 10^2$  are presented in fig. 3. The fluid is drawn towards the fin through the vertical

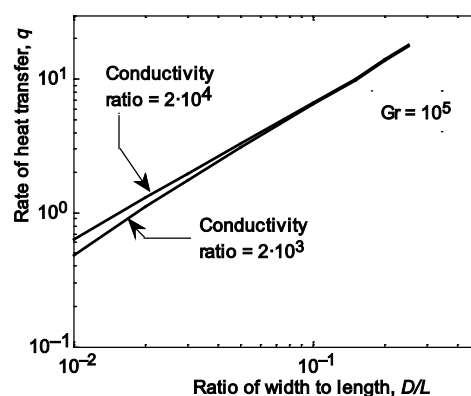


Figure 2. Effect of fin thermal conductivity

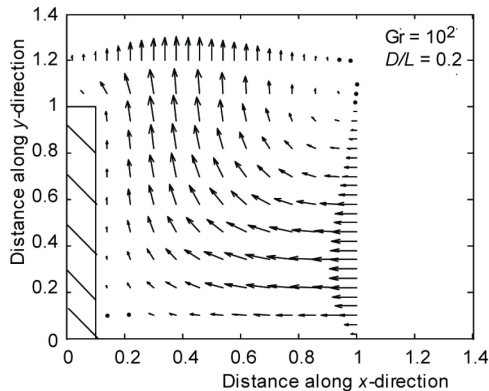


Figure 3. Velocity vectors for  $D/L = 0.2$  and  $Gr = 10^2$

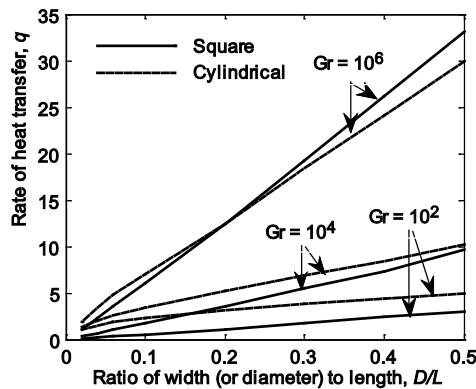


Figure 4. Effect of fin size on heat transfer

cylindrical fins are advantageous in spite of the fact that a cylindrical fin has about 27% lower surface area than a square fin. But the advantage diminishes with increasing fin diameter to length ratio as well as with increasing Grashof number. The former is due to decreasing curvature of the thermal boundary layer with increasing diameter of a cylindrical fin and the latter is due to decreasing thermal boundary layer thickness with increasing Grashof number [15]. It must be emphasized that for most practical applications, fin diameter to length ratio is below 0.2 and  $Gr$  below  $10^5$  for which the curvature effect of cylindrical fins on heat transfer is highly positive, fig. 4. Considering the large number of fins in a heat sink, the enhancement in absolute heat transfer with cylindrical fins over that with square fins can be substantial.

The increase in heat transfer with increasing fin width as seen in fig. 4 is at the expense of the fin occupying a larger area of the base plate. Consequently, a parameter of more practical importance is the heat flux at fin base rather than the total rate of heat transfer from the fin. With this in mind, fig. 5 has been plotted to observe the variation of base heat flux with fin width to length ratio and the trend is opposite to that in fig. 4 *i. e.* at a fixed Grashof number and fin length, base heat flux monotonically decreases with increasing fin width. Hence, large number of smaller width fins is more effective than fewer fins of bigger width occupying the same area of the base plate. Each profile is almost linear on a log-log scale and this helped to develop a correlation of the following form.

boundary which then gradually turns upwards as it approaches the fin and becomes almost vertical near the fin. Finally, the fluid leaves through the horizontal pseudo boundary at the top of the fin.

The effects of fin dimensions on heat transfer will be examined next. Figure 4 plots the rate of heat transfer against fin width (diameter for cylindrical fin) to length ratio for different values of Grashof number. For the purpose of comparison, the profiles for the case of cylindrical fin reported in Haldar [14] are also shown alongside. As width (or diameter) approaches zero indicating the condition of no fin, the rate of heat transfer also approaches zero for each of the profiles in the figure. At a particular width to length ratio of the fin, the rate of heat transfer increases with Grashof number for obvious reasons. Near linear variation of rate of heat transfer with fin width to length ratio for each profile supports the view advocated before that convection rather than conduction is the controlling mechanism since area associated with convection is proportional to the fin width while that for conduction is proportional to the square of the width. When comparison is made between square and cylindrical fins operating under equal Grashof number, the profiles reveal that

$$\text{Base heat flux, } q_b = 1.72 \text{ Gr}^{0.263} \left( \frac{D}{L} \right)^{-0.96} \quad (6)$$

The maximum deviation between the flux values predicted by the correlation and those from the numerical solution was found to be less than 7%. The above correlation is applicable to  $10^2 \leq \text{Gr} \leq 10^6$ ,  $0.02 \leq D/L \leq 0.5$  and fin to air thermal conductivity ratio equals to  $10^4$ . It may be underscored that the correlation provides heat flux at the base of the fin and excludes the contribution to heat transfer by the unfinned part of the plate.

The rate of heat transfer from a heat sink consists of contribution from each fin in the array and that from the free area of the plate. The heat flux calculated from eq. (6) multiplied by sum of the cross-sectional area of all the fins in the array provides contribution by the fins. While the contribution by the unfinned area of the plate may be determined from the available correlation for free convection from a upward facing horizontal surface [16], reproduced for ease of reference:

$$\text{Nu}^T = 0.835 \bar{C}_l \text{Ra}^{1/4}, \quad \text{Nu}_l = \frac{1.4}{\ln \left( 1 + \frac{1.4}{\text{Nu}^T} \right)}, \quad \text{Nu}_t = C_t^U \text{Ra}^{1/3},$$

$$\text{and finally } \text{Nu} = (\text{Nu}_l^m + \text{Nu}_t^m)^{1/m}$$

where  $\bar{C}_l = 0.671 / [1 + (0.492 / \text{Pr})^{9/16}]^{4/9}$ ,  $C_t^U = 0.140$ , and  $m = 10$ . The ratio of surface area to perimeter was chosen as the characteristic length in Rayleigh number and all the different forms of Nusselt numbers.

The rate of heat transfer so calculated may be regarded as the upper limit of free convection from a horizontal heat sink with square fins. The difference between the upper limit so calculated and the actual rate of heat transfer from a heat sink is expected to decrease with increasing gap between the fins in the array. It may be worth recalling that the optimum void fraction has been reported to be about 90%.

The rate of heat transfer [W] from an arbitrarily chosen heat sink has been calculated following the above procedure and plotted in fig. 6 as a function of base plate temperature [°C] above that of the free stream. The geometric details of the selected heat sink have been incorporated in the figure. Contributions to heat transfer by the fins is nearly twice of that by the free area of the plate though the fins occupy about 8% of the plate area.

In order to test the accuracy of the proposed method, comparison with the published results

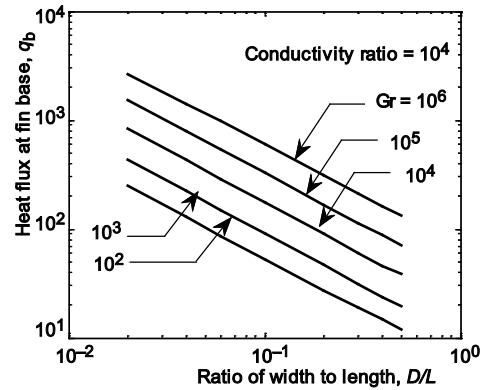


Figure 5. Heat flux at fin base with width to length ratio

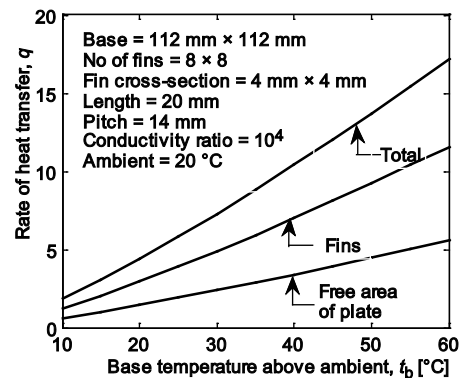


Figure 6. Heat transfer from a heat sink as a function of plate temperature

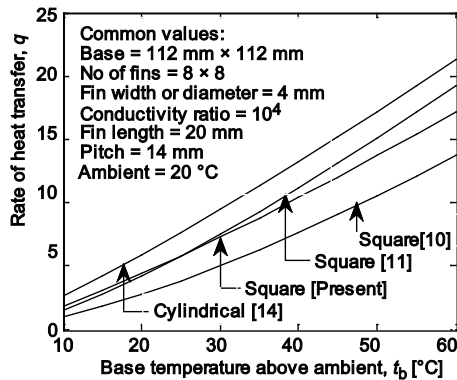


Figure 7. Comparison of heat transfer from heat sinks

has been shown in fig. 7 which plots the rate of heat transfer from a heat sink against the base plate temperature. Out of the four profiles in the figure, one was generated from the present results, two from the respective correlations provided by Huang *et al.* [10] and Sahray *et al.* [11] for heat sinks with square fins and the fourth one is from the correlation by Haldar [14] for a heat sink with cylindrical fins. The diameter of the cylindrical fins was chosen as equal to the width of the square fins of the other three cases. All the other geometric and operating parameters were kept identical and their values have been stated on the figure itself. The three correlations cited before are reproduced here for the sake of

completeness. For details on the applicability of these correlations the original articles may be referred to:

– Huang *et al.* [10]:

$$\xi = (0.0423 - 0.00493 \theta^{1.5}) Ra_w^{0.244+0.0051\theta^{2.5}} \sigma^{0.125-0.157\theta+0.05\theta^2} \varphi^{0.557-0.0192\theta^3}$$

where,  $Ra_w$  is the Rayleigh number based on width of the base plate as characteristic length,  $\theta$  – the orientation of the heat sink ( $\theta = 0$  for the present case of upward facing),  $\sigma$  – the finning factor defined as total surface area divided by the area of the base plate, and  $\varphi$  – the heat sink porosity defined as the ratio of fluid volume to the total volume.

– Sahray *et al.* [11]:

$$Nu_\delta = \frac{1}{30} \left( \frac{L}{D} \right)^{1/3} Ra_\delta^{1/2} \left[ 1 - \exp \left( - \frac{7000}{Ra_\delta} \right) \right]^{1/3}$$

where,  $D$  is the fin width and  $\delta$  the clear spacing between the fins. The exposed area in the definition of heat transfer coefficient in  $Nu_\delta$  is equal to the plate area plus the side area of all the fins in the heat sink.

– Haldar [14]:

$$q_b = a(D/L)^b$$

where,  $a = 2.658 Gr^{0.226}$  and  $b = -1.795 Gr^{-0.031}$  and  $q_b$  is the heat flux at the fin base. The contribution to heat transfer from unfinned part of the plate was obtained from Raithby and Hollands [16] as stated before.

Two of the four profiles, present and Haldar [14], predict the upper limit to free convection heat transfer while the other two, Huang *et al.* [10] and Sahray *et al.* [11], predict the actual heat transfer. The rate of heat transfer calculated from the correlation by Sahray *et al.* [11] is higher than that obtained from Huang *et al.* [10] by 40% at the lower plate temperature increasing to about 52% at higher temperatures. A significant part of the profile from Sahray *et al.* [11] is also above that obtained from the present results which are expected to be the upper bound of heat transfer. Accordingly the correlation by Sahray *et al.* [11] is believed to overestimate the rate of heat transfer. If compared with the results of Huang *et al.* [10], the rate of heat

transfer from the present method is higher by 88% at a plate temperature of 10 °C which gradually decreases to 25% at 60 °C for the chosen heat sink. This is quite reasonable considering the fact that the present correlation provides the upper bound. Poor convection current at low plate temperature may not reach the innermost fins of the heat sink and this renders the present results much higher than the actual. The difference between the heat transfer predicted by the proposed method and the actual is expected to diminish with the increasing gap between the fins.

The comparison between heat sink with square fins and that with cylindrical fins having diameter equal to the width of square fins reveals the advantage of the latter, fig. 7. For the case of the chosen heat sink, rate of heat transfer with cylindrical fins is expected to be 24% higher over that with square fins at a plate temperature of 10 °C and this value gradually increases to 40% at a plate temperature of 60 °C above the ambient establishing the superiority of cylindrical fins due to the curvature effect. It may be mentioned here that these values are dependent on the heat sink geometries.

## Conclusions

Laminar free convection about a single square fin attached to a horizontal base plate has been solved numerically and correlation has been developed to estimate heat transfer from square fin of any size and height. Single fin results have been then used to predict upper bound to free convection heat transfer from heat sinks. The results agree reasonably well with those reported in the literature. Heat flux at fin base almost linearly decreases with increasing fin width establishing the advantage of large number of slender fins over fewer fins of bigger size occupying the same area of the plate.

## Nomenclature

$A_p$  – free area of the base plate, [m<sup>2</sup>]  
 $A_{ex}$  – exposed area of a heat sink, [m<sup>2</sup>]  
 $D$  – width of a square fin or diameter of a cylindrical fin ( $d = D/L$ ), [m];  
 $g$  – acceleration due to gravity, [ms<sup>-2</sup>]  
 $Gr$  – Grashof number [ $= g\beta(T_b - T_o)L^3/\nu^2$ ], [-]  
 $k_{fin}$  – thermal conductivity of fin, [Wm<sup>-1</sup>K<sup>-1</sup>]  
 $k_{fluid}$  – thermal conductivity of fluid, [Wm<sup>-1</sup>K<sup>-1</sup>]  
 $L$  – length of fin, [m]  
 $Nu$  – Nusselt number  $\{= Q_p S / [(T_b - T_o) A_p k_{fluid}]\}$ , [-]  
 $Nu_o$  – Nusselt number  $\{= Q\delta / [(T_b - T_o) A_{ex} k_{fluid}]\}$ , [-]  
 $P$  – perimeter, [m]  
 $Pr$  – Prandtl number ( $= \nu/\alpha$ ), [-]  
 $Q$  – heat transfer rate,  $\{q = Q/[k_{fluid}(T_b - T_o)L]\}$ , [W]  
 $Q_b$  – heat flux at fin base  
 $\{q_b = Q_b/[k_{fluid}(T_b - T_o)L]\}$ , [W.m<sup>-2</sup>]  
 $Q_p$  – rate of heat transfer from a smooth plate, [W]  
 $Ra$  – Rayleigh number  $\{= g\beta[T_b - T_o]S^3/(\nu\alpha)\}$ , [-]

$Ra_o$  – Rayleigh number [ $= g\beta(T_b - T_o)\delta^3/(\nu\alpha)$ ], [-]  
 $S$  – ratio of surface area to perimeter, [m]  
 $T$  – temperature, [ $t = (T - T_o)/(T_b - T_o)$ ], [K]  
 $T_b$  – base temperature,  $t_b = 1.0$ , [K]  
 $T_o$  – free stream temperature,  $t_o = 0$ , [K]  
 $U$  – velocity along  $X$ , [ $u = U/(v/L)$ ], [ms<sup>-1</sup>]  
 $V$  – axial velocity, [ $v = V/(v/L)$ ], [ms<sup>-1</sup>]  
 $X$  – lateral co-ordinate, ( $x = XL$ ), [m]  
 $Y$  – axial co-ordinate, ( $y = Y/L$ ), [m]

### Greek symbols

$\alpha$  – thermal diffusivity, [m<sup>2</sup>s<sup>-1</sup>]  
 $\beta$  – volumetric coefficient of thermal expansion, [K<sup>-1</sup>]  
 $\delta$  – clear spacing between square fins, [m]  
 $\nu$  – kinematic viscosity, [m<sup>2</sup>s<sup>-1</sup>]  
 $\sigma$  – vorticity about  $Z$ ,  $\Omega = \sigma/(v/L^2)$ , [s<sup>-1</sup>]  
 $\Psi$  – stream-function,  $\psi = \Psi/v$ , [m<sup>2</sup>s<sup>-1</sup>]

## References

- [1] Kim, D. K., et al., Comparison of Thermal Performances of Plate-Fin and Pin-Fin Heat sinks Subject to an Impinging Flow, *Int. J. Heat Mass Transfer*, 52 (2009), Apr., pp. 3510-3517
- [2] Li, H. Y., et al., Performance Analysis of Pin-Fin Heat sinks with Confined Impingement Cooling, *IEEE Trans. on Components and Packaging Tech.*, 30 (2007), 3, pp. 383-389
- [3] Kim, D., et al., Compact Modeling of Fluid Flow and Heat Transfer in Pin Fin Heat sink, *J. Electronic Packaging, Trans. ASME*, 126 (2004), 3, pp. 342-350

- [4] Yang, K. S., et al., A Comparative Study of the Airside Performance of Heat sinks Having Pin Fin Configurations, *Int. J. Heat Mass Transfer*, 50 (2007), 23-24, pp. 4661-4667
- [5] Aihara, T., et al., Free Convective/Radiative Heat Transfer from Pin-Fin Arrays with a Vertical Base Plate (General Representation of Heat Transfer Performance), *Int. J. Heat Mass Transfer*, 33 (1990), 6, pp. 1223-1232
- [6] Zografos, A. I., Sunderland, J. E., Natural Convection from Pin Fin Arrays, *Experimental Thermal Fluid Sci.*, 3 (1990), 4, pp. 440-449
- [7] Sahray, D., et al., Study of Horizontal-Base Pin-Fin Heat sinks in Natural Convection, *Proceedings, IPACK2007 ASME InterPACK*, Vancouver, B. C., Canada, 2007
- [8] Kobus, C. J., Oshio, T., Development of a Theoretical Model for Predicting the Thermal Performance Characteristics of a Vertical Pin-Fin Array Heat sink under Combined Forced and Natural Convection with Impinging Flow, *Int. J. Heat Mass Transfer*, 48 (2005), 6, pp. 1053-1063
- [9] Sahiti, N., et al., Heat Transfer Enhancement by Pin Elements, *Int. J. Heat Mass Transfer*, 48 (2005), Avg., pp. 4738-4747
- [10] Huang, R. T., et al., Orientation Effect on Natural Convective Performance of Square Pin Fin Heat sinks, *Int. J. Heat Mass Transfer*, 51 (2008), 9-10, pp. 2368-2376
- [11] Sahray, D., et al., Study and Optimization of Horizontal-Base Pin-Fin Heat sinks in Natural Convection and Radiation, *J. Heat Transfer Trans. ASME*, 132 (2010), 1, pp. 012503-1-13
- [12] Leonard, B. P., Bounded Higher-Order Upwind Multidimensional Finite-Volume Convection-Diffusion Algorithms, in: *Adv. in Num. Heat Transfer*, 1 (Eds. W. J. Minkowycz, E. M. Sparrow), Taylor and Francis, Bristol, Penn, USA, 2000
- [13] Sharma, A., Eswaran, V., Conservative and Consistent Implementation and Systematic Comparison of SOU and QUICK Schemes for Recirculating Flow Computation on a Non-Staggered Grid, *Proceedings*, 2<sup>nd</sup> Int. and 29<sup>th</sup> National FMEP conf., Roorkee, India, 2002, pp. 351-358
- [14] Haldar, S. C., Natural Convection about a Cylindrical Pin Element on a Horizontal Plate, *Int. J. Thermal Sc.*, 49 (2010), 10, pp. 1977-1983
- [15] Cebeci, T., Laminar Free Convection Heat Transfer from the Outer Surface of a Vertical Slender Circular Cylinder, *Proceedings*, 5<sup>th</sup> International Heat Transfer Conference, Tokyo, 1974, pp. 15-19
- [16] Raithby, G. D., Hollands, K. G. T., Natural Convection, in: *Handbook of Heat Transfer*, (Eds. W. M. Rohsenow et. al.), 3<sup>rd</sup> edition, Ch. 4, McGraw Hill, N. Y., USA, 1998